Eur. Phys. J. A **28**, 301–306 (2006)
DOI 10.1140/epja/i2006-10056-2

THE EUROPEAN PHYSICAL JOURNAL A

Recoil-fission tagging of the transfermium nucleus ^{252}No

A.-P. Leppänen[1,a], J. Uusitalo[1,b], P.T. Greenlees[1], R.-D. Herzberg[2], N. Amzal[2], F. Becker[3,c], P.A. Butler[2], A.J.C. Chewter[2], J.F.C. Cocks[2], O. Dorvaux[1,d], S. Eeckhaudt[1], K. Eskola[4], J. Gerl[5], T. Grahn[1], N.J. Hammond[2], K. Hauschild[3,e], K. Helariutta[1,f], F.P. Heßberger[5], M. Houry[3,g], G.D. Jones[2], P.M. Jones[1], R. Julin[1], S. Juutinen[1], H. Kankaanpää[1,h], H. Kettunen[1], T.L. Khoo[6], W. Korten[3], P. Kuusiniemi[1,i], Y. Le Coz[3,j], M. Leino[1], C.J. Lister[6], R. Lucas[3], M. Muikku[1,k], P. Nieminen[1,l], M. Nyman[1], R.D. Page[2], J. Pakarinen[1], P. Rahkila[1], P. Reiter[7,m], J. Sarén[1], Ch. Schlegel[5], C. Scholey[1], O. Stezowski[8], Ch. Theisen[3], W.H. Trzaska[1], and H.J. Wollersheim[5]

[1] Department of Physics, University of Jyväskylä, FIN-40351, Jyväskylä, Finland
[2] Department of Physics, Oliver Lodge Laboratory, University of Liverpool, Liverpool L69 7ZE, UK
[3] DAPNIA/SPhN CEA-Saclay, F-91191 Gif-sur-Yvette Cedex, France
[4] Department of Physical Sciences, University of Helsinki, FIN-00014 Helsinki, Finland
[5] Gesellschaft für Schwerionenforschung, D-64220, Darmstadt, Germany
[6] Argonne National Laboratory, Argonne, IL, USA
[7] Ludwig Maximilians Universität, D-80539, München, Germany
[8] IPNL, 69622 Villeurbanne Cedex, France

Received: 16 March 2006 / Revised: 23 May 2006 /
Published online: 23 June 2006 –
Communicated by D. Schwalm

Abstract. An in-beam study of the transfermium nucleus ^{252}No has been performed using the JUROSPHERE II array of germanium detectors coupled to the gas-filled recoil separator RITU. A new technique of recoil-fission tagging was used to extract tagged γ-ray data. Having significant spontaneous fission and α-decay branches, ^{252}No is an ideal candidate for a comparative study. In a similar manner to α-decay tagging the fission events can be used to obtain γ-ray data. The recoil-fission tagged γ-ray spectrum showed a similar structure to the α-decay tagged γ-ray spectrum. By comparing the α-tagged and fission-tagged spectra and decay curves, it was shown that the spontaneous fission originates from the same initial state as the α decay. This extension of the tagging method allows in-beam spectroscopic data to be obtained from heavy nuclei with significant spontaneous-fission branches.

PACS. 25.70.-z Low and intermediate energy heavy-ion reactions – 25.85.Ca Spontaneous fission – 29.30.-h Spectrometers and spectroscopic techniques – 29.30.Kv X- and gamma-ray spectroscopy

1 Introduction

Nuclei far from stability are an important testing ground for the predictive power of nuclear models, and the investigation of the heaviest elements has always been one of the central themes of nuclear physics. The collected decay data establish a means of comparison with theoretical data. According to the liquid-drop model, nuclei with a proton number greater than approximately 102 should not exist. This is due to the destructive effect of Coulomb repulsion. However, the heaviest system reported to date contains 118 protons (see [1] and references therein). The

[a] *Present address:* Northern Finland Regional Laboratory, STUK - Radiation and Nuclear Safety Authority, Rovaniemi, Finland; e-mail: `leppanen@phys.jyu.fi`
[b] e-mail: `juha.uusitalo@phys.jyu.fi`
[c] *Present address:* Gesellschaft für Schwerionenforschung, D-64220, Darmstadt, Germany.
[d] *Permanent address:* IReS Strasbourg, IN2P3-CNRS, F-67037 Strasbourg, France.
[e] *Present address:* CSNSM, IN2P3-CNRS, F-91405 Orsay Campus, France.
[f] *Present address:* Department of Radiochemistry, University of Helsinki, 00014 Helsinki, Finland.
[g] *Present address:* DAM/DIF/DCRE, CEA Bruyères-le-Châtel, BP 12 - 91680 Bruyères-le-Châtel, France.
[h] *Present address:* Finnish Air Force, Tikkakoski, Finland.
[i] *Present address:* CUPP - Centre for Underground Physics in Pyhäsalmi, 86801 Pyhäjärvi, Finland.
[j] *Present address:* DEN/DTN/SMTM, CEA Cadarache, F-13108 Saint-Paul-lez-Durance Cedex, France.
[k] *Present address:* STUK - Radiation and Nuclear Safety Authority, Helsinki, Finland.
[l] *Present address:* Department of Nuclear Physics, The Australian National University, Canberra, Australia.
[m] *Present address:* IKP, Universität zu Köln, 50937 Köln, Germany.

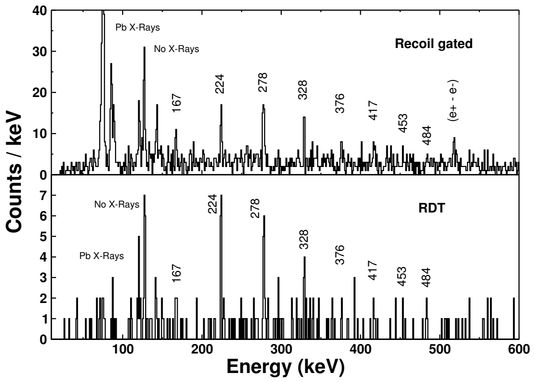

Fig. 1. Gamma-ray spectra obtained in the analysis of R.-D. Herzberg, where the method of recoil-α tagging was used. Upper panel: recoil-gated γ-ray spectrum. Lower panel: recoil-gated and ^{252}No α-tagged γ-ray spectrum. See ref. [10] for further details.

effect of shell stabilization accounts for the existence of super-heavy nuclei [2].

The heaviest systems are produced in fusion-evaporation reactions with cross-sections at or below picobarn levels. This means that no structure information can be obtained beyond α-decay energies, branching ratios or decay half-lives. Nuclei in the transfermium region can be produced with much higher cross-sections, at the microbarn or sub-microbarn level. At this level detailed nuclear spectroscopy can be performed using in-beam experiments, using the recoil-gating or recoil-decay tagging techniques. The techniques of recoil-gating and recoil-decay tagging, first used by Simon *et al.* [3] and Paul *et al.* [4], respectively, have been used with great success in recent years. A recent study of ^{254}No allowed excited states up to a spin of $22\hbar$ to be observed, and showed evidence for non-yrast states [5]. It is hoped that detailed knowledge of the structure of the transfermium elements will provide data to constrain nuclear models and aid predictions of the properties of super-heavy elements. Significant progress has been made in the study of transfermium nuclei lying around the "magic" deformed neutron sub-shell at $N = 152$ [5–7]. Today the heaviest nucleus for which in-beam spectroscopy has been performed is ^{255}Lr [8]. Many of the isotopes in the transfermium region have significant spontaneous-fission branches which compete with α decay. One can therefore extend in-beam spectroscopy to even heavier nuclei by tagging with fission events. One such example where recoil-fission tagging is essential in order to obtain γ-decay data is ^{256}Rf, which has a spontaneous-fission branch of 99.5% [9].

The detection efficiency for α particles is around 55%, as a large fraction of the emitted α particles escape the detector into which the recoils are implanted. The absolute value of the detection efficiency is dependent on the α-particle energy and implantation depth. In the case of fission, the fragments are emitted back-to-back and it is enough to detect one of the fragments. This means that the fragments are detected with much higher efficiency. The main technical problem in detecting both α particles and fission fragments simultaneously is the huge difference in decay energies. Alpha-decay energies are of the order of 5–10 MeV while the total kinetic energy release (TKE) in fission is of the order of 200 MeV.

The data obtained in the experiment described in this work were previously analysed using the recoil-gating and recoil-(α)-decay tagging techniques by Herzberg *et al.*, and published in ref. [10]. Figure 1 shows the γ-ray spectra obtained in the analysis presented therein. The spontaneous-fission branch of ^{252}No is around 20–25% with a total production cross-section of around 220 nb with a half-life of $T_{1/2} = 2.3(2)$ s [11]. This makes ^{252}No an ideal case for a comparative study of fission and α-decay tagging. In this work a proof-of-principle analysis of the recoil-fission tagging of ^{252}No is presented.

2 Experimental details

The experiment was carried out at the Accelerator Laboratory of the University of Jyväskylä using the JUROSPHERE II germanium detector array coupled to the gas-filled recoil separator RITU [12]. The JUROSPHERE II comprised 27 Compton-suppressed HPGe detectors (15 Eurogam Phase I, 5 Nordball and 7 Tessa) [13–15]. The total photopeak efficiency was 1.7% at 1.3 MeV. The reaction $^{206}\mathrm{Pb}(^{48}\mathrm{Ca}, 2\mathrm{n})^{252}\mathrm{No}$ was employed to produce ^{252}No. The beam energy at the center of the target was 216 MeV corresponding to an average excitation energy of 22.5 MeV. The targets were 500 μg/cm^2 thick self-supporting foils of ^{206}Pb produced from isotopically enriched material containing 99.8% ^{206}Pb. The total beam dose of ^{48}Ca particles incident on the target was approximately 9.3×10^{16}. The experimental details are summarized in table 1.

A position-sensitive PIPS (Passivated Implanted Planar Silicon) detector was used at the focal plane of RITU to identify recoils and their subsequent decays and also as a start detector for the time-of-flight (TOF) measurement. The PIPS detector has sixteen individual position-sensitive strips. The size of the detector was 80×35 mm^2. Individual energy signals were taken from the top and bottom of each PIPS strip. These signals were used to determine the position of an event, through charge division. In addition, the top and bottom signals were used to determine the total energy of an event. There were two methods

Table 1. Summary of experimental details.

Beam	$^{48}\mathrm{Ca}^{9+}$
Beam energy (E_{CoT})	216 MeV
Excitation energy (E^*)	22.5 MeV
Target	^{206}Pb
Target thickness	500 μg/cm^2
Irradiation time	238 h
Approximate total dose	9.3×10^{16} part.

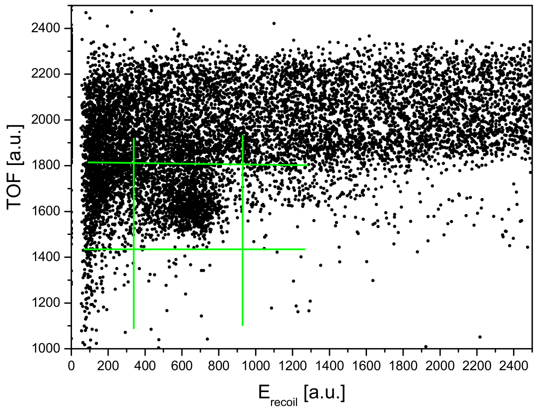

Fig. 2. Time of flight *versus* recoil energy. The gates used to select ^{252}No recoils are shown in the figure.

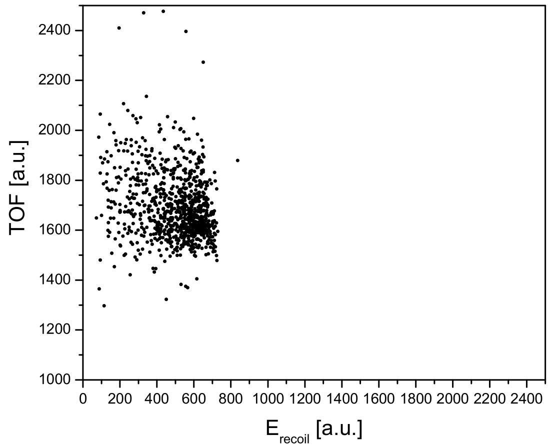

Fig. 3. Events found to correlate with ^{252}No α decay shown in a recoil energy *versus* time-of-flight plot.

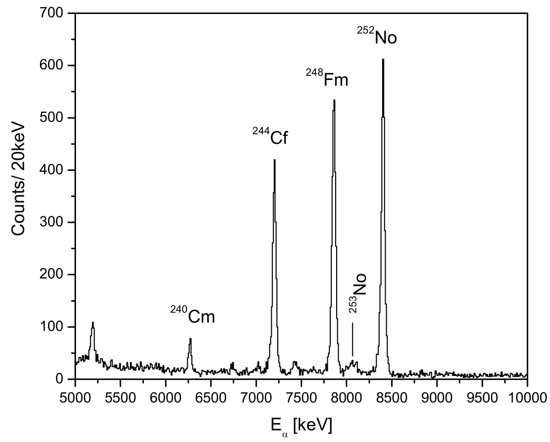

Fig. 4. Partial spectrum of events in the PIPS detector, in anti-coincidence with the MWPC. The α-decay peaks of interest are labelled.

to determine the total energy. The first method involved the electronics associated with the PIPS detector. The individual top and bottom signals were fed into a sum amplifier to give the total energy. In the second method, the individual top and bottom signals were summed in software during the offline analysis. In the figures shown here, the software total energy is labelled as "rec sum plus". The software total energy has poor energy resolution but extends the detectable energy range significantly. In addition to the PIPS detector, the focal-plane spectrometer of RITU also consisted of a Multi-Wire Proportional Counter (MWPC) and four Nordball-type HPGe detectors. The MWPC used gold-plated tungsten wires with 1 mm pitch in x- and y-direction. The operational voltage of the MWPC was 450 V. Two different signals were taken from the MWPC, an energy loss signal (ΔE) and a stop signal for the time-of-flight measurement.

A total of 2890 α decays with full energy from the ground state of ^{252}No and 1440 ^{252}No fission events were identified. A more detailed description of the experiment can be found in ref. [10].

3 Analysis

As mentioned above, the analysis of ^{252}No γ-ray data based on recoil-gating and recoil-α-decay tagging was reported in ref. [10]. The analysis did not include the tagging of recoils with fission events, which is addressed here. The first step in the analysis is the identification of recoils. The ^{252}No recoils can be identified from matrices of the time of flight *versus* recoil energy and energy loss in the MWPC *versus* the recoil energy. As the flight distance between the PIPS detector and the MWPC was only 10 cm, the beam and the recoils are not clearly separated. Figure 2 shows a plot of the time of flight *versus* the recoil energy. The gates used to select ^{252}No recoils are also shown in the fig. 2. With a beam energy of 216 MeV essentially only the 2n evaporation channel was open, which can be seen from fig. 4 where ^{252}No α decay clearly dominates. The other strong peaks (^{248}Fm, ^{244}Cf and ^{240}Cm) belong to the ^{252}No decay chain.

Figure 3 shows a plot where recoils were correlated with ^{252}No α decay with open recoil energy and time-of-flight gates with the execption $E_{\mathrm{recoil}}[\mathrm{a.u.}] < 1000$. In fig. 3 the ^{252}No recoils form the majority of the correlated events but some scattered beam is still present. The scattered-beam component can be minimized by optimizing the gates around these events and following the effect on the recoil-(α)-tagged γ spectrum.

Figure 4 shows the partial α particle energy spectrum in anti-coincidence with the MWPC. The anti-coincidence with MWPC separates the actual ^{252}No α decays from the scattered low-energy beam particles.

The selected recoils shown in fig. 2 were found to correlate with the ^{252}No α peak, presented in fig. 4 within four

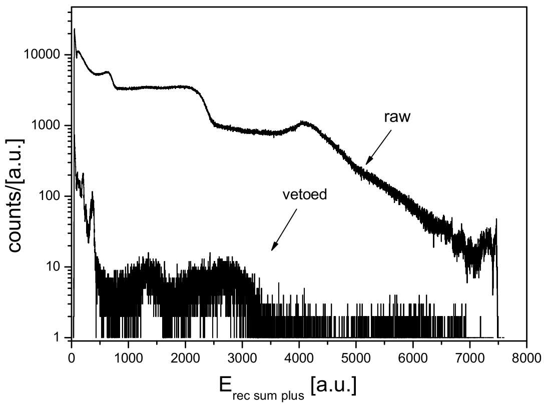

Fig. 5. Low-gain amplification energy spectrum where the individual top and bottom signals of the PIPS detector were summed in software to create a new total energy. "raw" represents all events and "vetoed" represents events in anti-coincidence with the MWPC detector. The figure shows partial data.

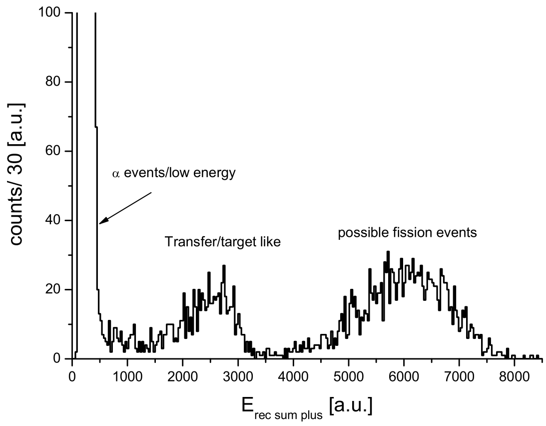

Fig. 6. Spectrum of events in the low-gain amplification range position and time correlated with ^{252}No recoils within a maximum search time of 15 s. Individual top and bottom signals were summed in software to create a new total energy. The figure contains all data from the experiment.

half-lives (10 s) [11] time interval after the implantation of a recoil and within a position window of 1.7 mm.

3.1 Detection of fission events

The PIPS detector was instrumented with two separate amplification channels in order to maintain resolution for low-energy events, and to allow simultaneous detection of high-energy events. The high-gain amplification channel was used for signals from low-energy events such as α decay. The low-gain amplification channel was used for high-energy signals such as the implantation of a recoil or a fission event. The two gain ranges overlapped such that high-energy α decays could also be seen in the low-gain amplification range. As described earlier, the signals taken from the top and bottom of the PIPS detector were fed into a sum amplifier to create a total energy signal. Unfortunately, the gain of the low-amplification range was tuned such that fission events had a high probability of saturating the sum amplifier. To overcome this limitation, the individual top and bottom signals were summed in software in order to measure the fission events with very high decay energy. This method extended the dynamic range of the low-amplification side and allowed fission events to be distinguished. Figure 5 shows the low-gain amplification energy spectrum produced through software summing of the individual top and bottom signals. If the software summing of the individual top and bottom signals is not used, the spectrum is cut off at around channel number 4000. In the figure "raw" represents all events and "vetoed" represents events in anti-coincidence with the MWPC detector.

In the process of searching for fission events a temporal and spatial correlation was made between ^{252}No recoils and events in the low-gain amplification range. The maximum search time allowed for the correlation was 15 s, which corresponds to six half-lives. No energy constraints were placed on events in the low-gain amplification range. Figure 6 shows the resulting correlated spectrum from the low-gain amplification range. Two broad distributions appear in the total energy spectrum. The broad distribution at channel numbers 2000–3000 represents target-like transfer or knock-out products which were not triggered (vetoed) by the MWPC. The pulse-height defect (PHD) distorts the total energy scale since it is dependent on both mass and energy. Fission fragments typically have masses $M = 100$–150 and energies $E = 0.5$–$1.5\,\mathrm{MeV/u}$ while transfer products in this case have masses close to the target mass of typically $M = 206$–210 and energies $E \approx 0.6\,\mathrm{MeV/u}$. In this respect the PHD is higher for transfer products. This does not pose a significant problem since the energy estimation is very rough and provides a region of interest rather than an accurate calibration. Taking the energy loss in all materials within RITU into account, the target-like products should have energies of the order of 70 MeV. The centroid energy of the broad distribution at higher channel numbers therefore corresponds to roughly 160 MeV. Thus, the broad distribution at channel numbers 5000–7000 represents the possible ^{252}No fission events.

Figure 7 shows the number of observed decay events as a function of time plotted for both the ^{252}No α-decay events and the assumed ^{252}No fission events. When the decay curve of the presumed ^{252}No fission events was compared with the ^{252}No α-decay curve a similar behavior was observed.

The resulting half-lives extracted from these curves were $T_{1/2} = (2.46 \pm 0.05)$ s for the ^{252}No α decay and $T_{1/2} = (2.54 \pm 0.07)$ s for the assumed ^{252}No fission events. Within the error limits the observed half-lives are in agreement with the previously measured value 2.3(2) s [11]. This gives strong support to the assumption that the broad dis-

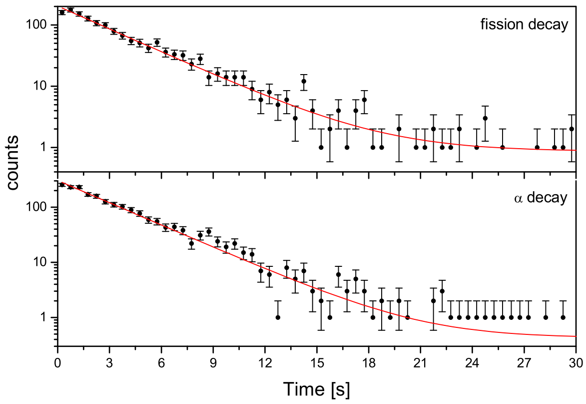

Fig. 7. Upper part: Decay curve of the assumed ^{252}No fission events. Lower part: Decay curve of the ^{252}No α-decay events. A half-life of $T_{1/2} = (2.54 \pm 0.07)$ s was deduced for the fission events and a half-life of $T_{1/2} = (2.46 \pm 0.05)$ s for the ^{252}No α decay. Within error limits the half-lives are identical.

tribution of high-energy events, shown in fig. 6, does indeed represent ^{252}No fission events. Further support can be obtained from the γ-ray spectrum. If the assumed fission events produce a similar tagged γ-ray spectrum as that obtained with α-decay tagging, it can be stated with conviction that the broad distribution represents real ^{252}No fission events.

3.2 Recoil-α and recoil-fission tagging

In recoil-decay tagging experiments, as each recoil is implanted into the position-sensitive implantation detector, all γ-rays in coincidence with the recoil implant are stored. A search is then made for recoil-decay pairs at the same position in the detector within a given search time, this technique is called recoil-gating [3]. The search time varies from one experiment to another and it is dependent on the background counting rate (typically a few half-lives of the decay in question). The γ-rays associated with such recoil-decay pairs are then incremented into a spectrum, this technique is called recoil-decay tagging [4]. In the case of ^{252}No both α decay and fission events can be used to tag γ-rays.

The γ-ray spectra obtained through recoil-fission tagging and recoil-α tagging are shown in fig. 8. The upper panel shows the γ-ray spectrum corresponding to correlated recoil-fission pairs found at the same position in the implantation detector within a search time of 15 s. The selected fission events are those in channels 4700 to 7500 shown in the spectrum in fig. 6. The corresponding recoil-α decay-tagged spectrum is shown in the middle panel. This spectrum is almost identical to the lower panel in fig. 1 which was obtained in the original analysis of Herzberg *et al.*. In both the recoil-fission and recoil-α tagged spectra the yrast rotational sequence of ^{252}No can be clearly seen. The lower panel in fig. 8 shows a summed γ-ray spectrum of those events from both the recoil-fission and recoil-α tagging analysis. The advantage of using both

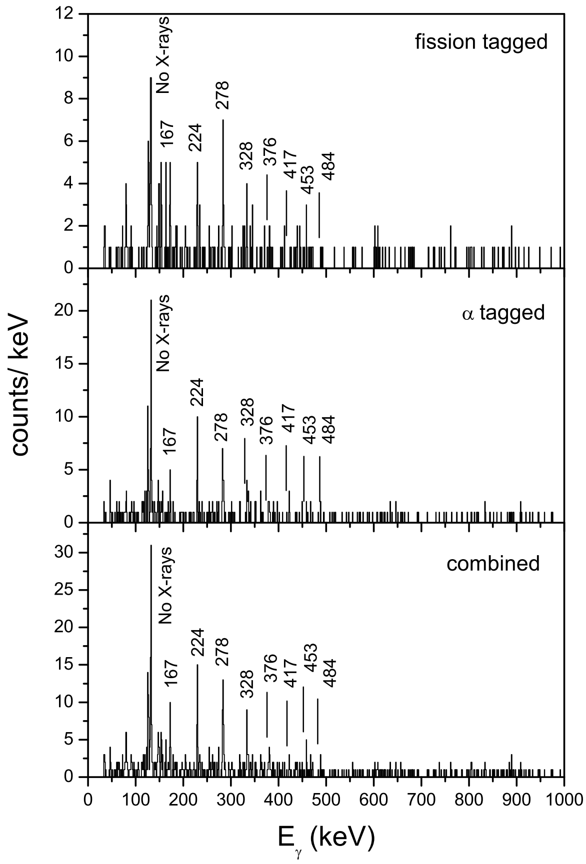

Fig. 8. Upper panel: γ-ray spectrum obtained through tagging with ^{252}No fission events. Middle panel: γ-ray spectrum obtained through tagging with the ^{252}No α decay. Bottom panel: summed γ-ray spectrum from both recoil-fission and recoil-α tagged events.

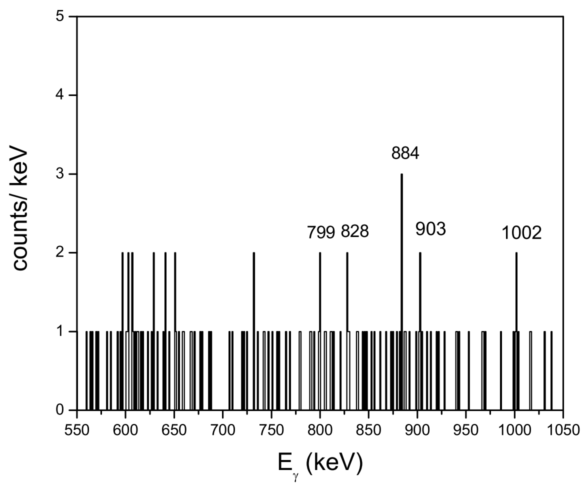

Fig. 9. Candidates for new transitions at the high-energy part of the combined recoil-α and recoil-fission tagged γ-decay spectrum.

tagging techniques can be seen, as the rotational band sequence is much more pronounced, and the in-band intensity ratios closer to those of the recoil-gated spectrum shown in fig. 1. A further advantage of using the summed spectrum can be seen in fig. 9, where an expansion of the high-energy part of the combined γ-ray spectrum is shown.

In fig. 9, several candidates for high-energy peaks can be seen, which are not visible in either the recoil-gated or recoil-α tagged spectra. It is assumed that these peaks correspond to transitions from high-lying non-yrast states, similar to those recently observed in ^{254}No [5]. Further support for this interpretation comes from data recently obtained using the velocity filter SHIP at GSI and fragment mass analyser (FMA) at ANL. In those experiments delayed γ-rays with similar-energies have been observed to originate from ^{252}No [16,17].

3.3 Alpha-decay and spontaneous-fission branching ratios

The relative α-decay and spontaneous-fission branching ratios can be determined on the basis of our data. A total of 2890 ^{252}No α-decay events were detected, along with a total of 1440 ^{252}No fission events. The observed values must be corrected for the relevant detection efficiencies. In the case of α decay the detection efficiency is 55% whilst for fission fragments the detection efficiency is approximately 90%. The detection efficiency for fission fragments is geometric, and is determined by the solid angle into which a fission fragment escapes from the detector and triggers the MWPC. All events where the fission fragment does not trigger the MWPC are considered to be detected, resulting in a value of 90%. After applying corrections for the relative detection efficiencies the total number of α decays was 5250 and the total number of fission events was 1620. From this the ratio of α-decay/SF can be determined as $\alpha/\mathrm{SF} = 3.3(8)$. This is in agreement with previously reported values of $\alpha/\mathrm{SF} = 2.7$ [11] and $\alpha/\mathrm{SF} = 3.6$ [18]. A recently published study reported a fission branch of $b_{\mathrm{SF}} = (32 \pm 3)\%$ [19].

4 Summary

Fission events at the focal plane of RITU were analyzed for the first time, and the new recoil-fission tagging method was employed to obtain γ-ray spectra for ^{252}No. The identical α-decay and fission half-lives prove the successful identification of spontaneous fission of ^{252}No. The identical yrast rotational band structure in the recoil-α and recoil-fission tagged γ-ray spectra demonstrates the feasibility of the recoil-fission tagging method. The simultaneous detection of α decay and spontaneous-fission events provided direct access to the relative branching ratios. The measured ^{252}No α decay and fission branching ratios were found to agree with previously published values.

From the combined γ-ray spectrum, an increase in statistics of approximately 50% over the recoil-α tagged spectrum can be seen. The highest-energy transitions (those with lower statistics) are more clear and the transitions having the highest γ-ray energy can be confirmed. At the higher energies, above 500 keV, there are candidates for non-yrast transitions, as seen in the neighboring even-even isotope ^{254}No. Due to a lack of statistics and γ-γ coincidences the identification of possible non-yrast peaks is difficult and no firm conclusions concerning the decay scheme can be drawn.

References

1. Yu.Ts. Oganessian *et al.*, Phys. Rev. C **70**, 064609 (2004).
2. W.D. Myers, W.J. Swiatecki, Nucl. Phys. **81**, 1 (1966).
3. R.S. Simon *et al.*, Z. Phys. A **325**, 197 (1986).
4. E.S. Paul *et al.*, Phys. Rev. C **51**, 78 (1995).
5. S. Eeckhaudt *et al.*, Eur. Phys. J. A **26**, 227 (2005).
6. R.-D. Herzberg *et al.*, J. Phys. G **30**, R123 (2004).
7. P.T. Greenlees *et al.*, Eur. Phys. J. A **20**, 87 (2003).
8. P.T. Greenlees *et al.*, to be published.
9. F.P. Heßberger *et al.*, Z. Phys. A **359**, 415 (1997).
10. R.-D. Herzberg *et al.*, Phys. Rev. C **65**, 014303 (2001).
11. C.E. Bemis jr. *et al.*, Phys. Rev. C **15**, 705 (1977).
12. M.E. Leino *et al.*, Nucl. Instrum. Methods B **99**, 653 (1995).
13. C.W. Beausang *et al.*, Nucl. Instrum. Methods A **313**, 37 (1992).
14. B. Herskind, Nucl. Phys. A **447**, 395 (1985).
15. P.J. Nolan, D.W. Gifford, P.J. Twin, Nucl. Instrum. Methods A **236**, 95 (1985).
16. F.P. Heßberger *et al.*, Int. J. Mod. Phys. **15**, 284 (2006).
17. A. Robinson *et al.*, to be published.
18. A.N. Andreyev *et al.*, Z. Phys. A **345**, 389 (1993).
19. A.V. Belozerov *et al.*, Eur. Phys. J. **16**, 447 (2003).